Braz J Phys (2014) 44:223–232
DOI 10.1007/s13538-014-0181-2

SOCIEDADE BRASILEIRA DE FÍSICA

CONDENSED MATTER

Quantum Interference Effects for the Electronic Fluctuations in Quantum Dots

J. G. G. S. Ramos · A. L. R. Barbosa · M. S. Hussein

Received: 23 May 2013 / Published online: 25 March 2014

Abstract For the main quantum interference term of coherent electronic transport, we study the effect of temperature, perpendicular and/or parallel magnetic fields, spin-orbit coupling and tunneling rates in both metallic grains and mesoscopic heterostructures. We show that the Zeeman effects determines a crucial way to characterize the quantum interference phenomena of the noise for anisotropic systems (mesoscopic heterostructures), qualitatively distinct from those observed in isotropic structures (metallic grains).

Keywords Charge transport · Mesoscopic systems · Thermal noise

1 Introduction

A two-dimensional electron gas can provide a myriad of possibilities for manipulating electronic degrees of freedom. Recent advances show that it is possible to control its spin, orbital and charge degrees of freedom through magnetic fields, and crystal asymmetries of two-dimensional quantum dot (QD) structures [1–3]. Experimental realizations of the QD can be metallic grains or mesoscopic heterostructures of various kinds. The statistical properties of the electronic transport in ballistic open QDs have been intensively studied over the last decades [4, 5]. In such systems, the conductance can be described by the Landauer formula and, for QDs containing a large number of electrons, the random matrix theory (RMT) provides an excellent statistical description of the underlying chaotic electronic dynamics at the Fermi energy [5, 6]. Such a control of the QD permits studying confinement effects just as the quantum interference between injected electrons [7]. External parameters govern these quantum interferences, which is essentially affected by the time-reversal (TRS) and spin-rotation (SRS) symmetries of the universal quantum transport [8]. There are three Wigner-Dyson universal ensembles, namely circular orthogonal ensemble (COE), which is characterized by the presence of TRS and SRS ($\beta = 1$), circular unitary ensemble (CUE), which has the TRS broken by external magnetic field ($\beta = 2$), and circular symplectic ensemble (CSE), which is characterized by both TRS and SRS broken by a spin-orbit interaction ($\beta = 4$). The finite fields and/or finite spin-orbit coupling can generate a crossover (intermediate case) between the universal classes of Wigner-Dyson.

It is widely known in the literature that a perpendicular magnetic field breaks time reversal symmetry, leading the QD from orthogonal to unitary ensembles. On the other hand, the spin-orbit coupling breaks the spin rotational symmetry, making the crossover to the symplectic ensemble. One of the main signatures of the spin-orbit coupling is the presence of an anti-localization term in the conductance,

J. G. G. S. Ramos · M S Hussein (✉)
Instituto de Estudos Avançados, Universidade de São Paulo,
C.P. 72012, 05508-970 São Paulo, SP, Brazil
e-mail: hussein@if.usp.br

J. G. G. S. Ramos · M S Hussein
Instituto de Física, Universidade de São Paulo,
C.P. 66318, 05314-970 São Paulo, SP, Brazil

J. G. G. S. Ramos
Departamento de Ciências Exatas, Universidade Federal
da Paraíba, 58297-000, Rio Tinto, PB, Brazil

A. L. R. Barbosa
UAEADTec and Pós-Graduação em Física Aplicada,
Universidade Federal Rural de Pernambuco,
52171-900, Recife, PE, Brazil

i.e., an amplification of the signal in addition to semiclassical term [9, 10]. A magnetic field suppresses this quantum interference correction and, in particular, the localization signal [11]. In other studies, it was shown that the scattering mechanisms with the combined effect of spin-orbit coupling and Zeeman effect (caused by a magnetic field parallel to the two-dimensional electron gas) can generate a rich class of crossovers between regimes of localization and anti-localization [12–14]. Therefore, the Zeeman effect plays a role similar to a perpendicular magnetic field [15].

Fluctuation properties of the nonequilibrium current injected in QD indicate that just the average charge conductance are not enough for a complete description of the full quantum transport [2, 3]. In the limit of high temperatures, Johnson-Nyquist noise provides information on the thermal fluctuations, a fingerprint of dissipative systems. On the other hand, experimental measurements of noise at low temperatures, also known as shot-noise, use tunneling rate in the nonideal quantum transport [1], yielding important information about the discrete process of charge transmission [16]. In mesoscopic systems, both noise sources are present.

In the presence of only perpendicular magnetic field and spin-orbit coupling, both the conductance and the shot-noise power of a metallic grain and a GaAs-type heterostructure are indistinguishable [11], i.e., have the same qualitative behavior in its two main cumulants of the full counting statistics, conductance, and noise. A metallic grain has a spin-orbit coupling a (defined below) determined at the atomic level. On the other hand, heterostructures have spin-orbit coupling determined by its band structures (such as in GaAs) or by a nonsymmetric confinement (such as in GaAs/AlGaAs interfaces), depending on the parameters a and $a_\perp$ defined below.

Physical effects almost identical in seemingly different systems invite one to raise questions concerning interference phenomena in conductante and quantum noise for anisotropic systems (mesoscopic heterostructures), qualitatively different from those observed in isotropic structures (metallic grains). As we analytically show, the Zeeman effect induced by a parallel magnetic field can establish such separation criterion. More specifically, the phenomenological signal that distinguishes the two alluded systems appears more strongly in the noise, and very weakly in the conductance, only in the presence of the Zeeman parallel magnetic field. Another mechanism that can establish the criterion, together with the Zeeman field, is the thermal crossover proposed in [25] to suppress the depletion-amplification effect in the interference correction of the noise. The depletion-amplification effect is a change in the signal (positive or negative) of the weak-localization term in the noise determined essentially by barriers (tunneling rates). With the combined effects, the two classes of systems become distinguishable as the plots in Figs. 1, 2, 3, 4 and 5 will show.

The system to be studied is depicted in Fig. 1. It consists of a chaotic quantum dot connected to two electron reservoirs via ideal leads with a number of open channels. The electron reservoirs have temperature T and electrochemical potentials $\propto_1$ and $\propto_2$ generating a potential difference eV. The entrance and exit tunneling rates through the barriers are Γ_1 and Γ_2, respectively. The QD can couple the spin and orbital degrees of freedom through relativistic corrections owing to the band structure and/or asymmetries in interfaces of heterostrutures and through a parallel magnetic field in the two-dimensional gas. Meanwhile, for metallic grains, only atomic relativistic corrections can couple spin and orbital degrees of freedom. Quantum interference effects are considered for a QD of

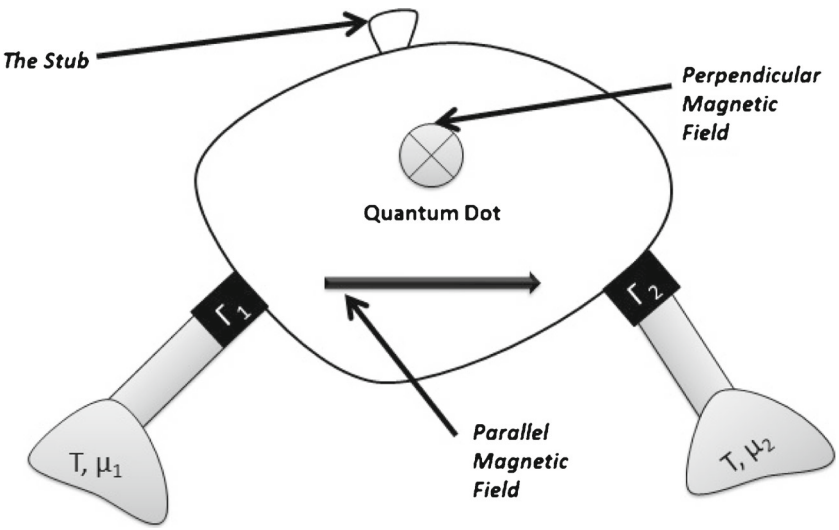

Fig. 1 The figure exhibits a quantum dot (*QD*) connected to reservoirs (source and drain) of electrons at a finite temperature. To the quantum dot is applied parallel and perpendicular magnetic fields. The effect of all fields generates an effective amplification of the phase space within the QD and can be incorporated through a fictitious stub connected to the QD geometry

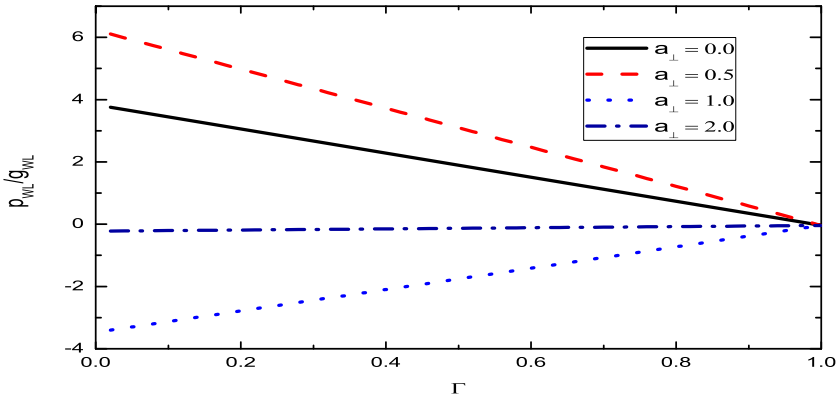

Fig. 2 Ratio p_{wl}/g_{wl} between "weak localization" (*WL*) terms for noise and conductance as a function of symmetric contacts

both types and, as we shall show, this differences is of crucial importance for the noise, which exhibits interesting Zeeman effects.

2 Scattering Theory of Quantum Transport

We consider the system depicted in Fig. 1, the standard setting of a two-probe open quantum dot coupled by leads to a source and to a drain electronic reservoir. We also assume that the source (drain) reservoir is coupled to the quantum dot by a lead that has N_1 (N_2) open modes (resulting from perpendicular Schrödinger quantization on the leads). The scattering matrix S describing the electron flow is given by [5]

$$S = \begin{pmatrix} r & t \\ t' & r' \end{pmatrix}, \tag{1}$$

here r (r') is the $N_1 \times N_1$ ($N_2 \times N_2$) matrix containing the reflection amplitudes of scattering processes involving channels at the source (drain)-coupled leads, while t (t') is the $N_1 \times N_2$ ($N_2 \times N_1$) matrix built by the transmission amplitudes connecting channels that belong to the source-coupled lead to the modes at the drain-coupled lead (and vice versa).

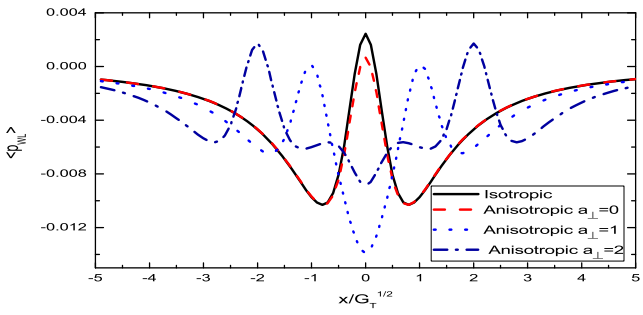

Fig. 3 Weak localization (*WL*) correction to shot-noise power term as a function of perpendicular magnetic field

In the chaotic regime, the mean free path l and the linear size of the dot L satisfy the relation $l << L$. The characteristic time scale in this regime is τ_D, the time for the electron to diffuse along the dot, also called dwell time. The corresponding energy scale is known as Thouless energy $E_T = \hbar/\tau_D$. In the universal regime, we assume all the time scales to be much greater than Ehrenfest time, that is, the QD is sufficiently large to ensure the semiclassical regime. In the universal regime, we calculate the conductance at zero temperature and the noise at finite temperature. Firstly, at zero temperature, the linear conductance G of an open QD is given by the Landauer formula

$$G = \frac{2e^2}{h}\mathcal{T} \;\; with \;\; \mathbf{g} = \mathbf{Tr}\left(t^\dagger t\right), \tag{2}$$

where the factor 2 accounts for spin degeneracy and $\mathbf{g}$ is the dimensionless conductance or transmission coefficient of the electron with charge e, which depends on N_1, N_2, the quantum dot geometry (see Fig. 1), the external fields, the QD impurities, etc. We assume also the *linear regime* on the Landauer approach, that is, we assume the validity of the relation $eV/(k_BT) << 1$, i.e., the linear response regime.

We start [16] by considering the time-dependent current $\hat{I}_\gamma(t)$ at lead γ, for $\gamma = 1, 2$. Within the framework of the scattering theory for quantum transport, the current-current correlation function can be written in the form [16]

$$\langle \delta\hat{I}_\alpha(t)\delta\hat{I}_\beta(0)\rangle = \int \frac{dw}{2\pi} e^{-iwt}\boldsymbol{\mathcal{S}}_{\alpha\beta}(\omega), \tag{3}$$

where $\delta\hat{I}_\alpha(t) \equiv \hat{I}_\alpha(t) + \langle\hat{I}_\alpha(t)\rangle$ is the current fluctuation around the mean value $\langle\hat{I}_\alpha(t)\rangle$. The Fourier transform of the current-current correlation function, (3), namely $\boldsymbol{\mathcal{S}}_{\alpha\beta}(\omega)$, is the noise, which for only a DC current can be written as follows:

$$\boldsymbol{\mathcal{S}}_{\gamma\alpha}(0) = \sum_{\nu,\rho}\frac{e^2}{h}\int d\varepsilon\, \mathbf{Tr}\left[A_{\rho\gamma}(\varepsilon)A_{\nu\alpha}(\varepsilon)\right] \times \left\{f_\nu(\varepsilon)\left[1 - f_\rho(\varepsilon)\right] + f_\rho(\varepsilon)\left[1 - f_\nu(\varepsilon)\right]\right\} \tag{4}$$

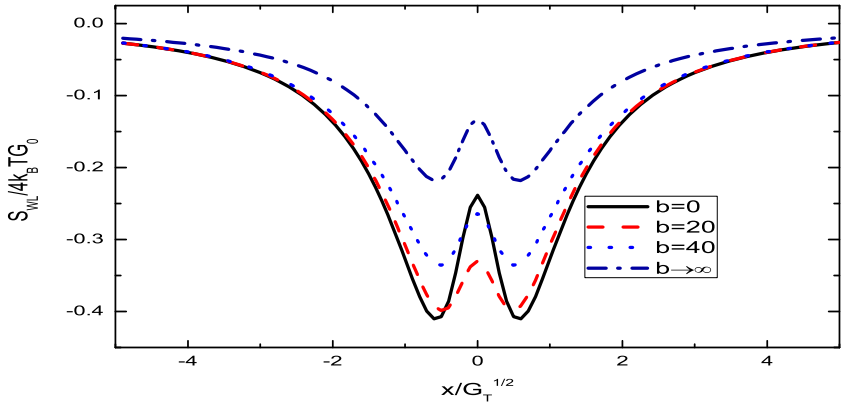

Fig. 4 Interference correction for the noise as a function of perpendicular magnetic field for finite b

The matrix $A_{v\alpha}(\varepsilon) = 1_\alpha 1_v - 1_v S^\dagger(\varepsilon) 1_\alpha S(\varepsilon)$ is the current matrix, where $S(\varepsilon)$ is the scattering matrix and $f_\gamma(\varepsilon)$ represents the Fermi distribution function.

The scattering matrix $S(\varepsilon)$ used to describe the mesoscopic system is uniformly distributed over the orthogonal ensemble, if the system has both time-reversal and spin rotation symmetry, over the unitary ensemble, if only time-reversal symmetry is broken by a intense external magnetic field, or over the symplectic ensemble, if the spin rotation symmetry is broken by a intense spin-orbit interaction [17]. We are interested in the correlation function for the currents in leads 1 and 2 together. The scattering matrix is uniform within an energy window in the vicinity of Fermi level. Henceforth, we will calculate the noise for this correlation function, i.e., the function $\boldsymbol{\mathcal{S}} \equiv \boldsymbol{\mathcal{S}}_{12}$.

For $k_B T \gg eV$, the current fluctuations are dominated by the thermal Johnson-Nyquist noise resulting in $\boldsymbol{\mathcal{S}} = 4k_B T G_0 \mathbf{Tr}\left(tt^\dagger\right)$, where $G_0 = e^2/h$ is the quantum conductance. On the other hand, for temperature much lower than the bias tension, $eV \gg k_B T$, the current fluctuations are dominated by the shot-noise power, $\boldsymbol{\mathcal{S}} = G_0\left[\mathbf{Tr}\left(tt^\dagger\right) - \mathbf{Tr}\left(tt^\dagger\right)^2\right]$. At finite temperature, both the thermal noise and the shot-noise power contribute to the fluctuations. The thermal crossover between the two kind of noise can be obtained [18, 19] from (4)

$$\frac{\boldsymbol{\mathcal{S}}\left(k_B T, eV\right)}{4k_B T\ G_0} = \mathbf{Tr}\left(tt^\dagger\right)^2 + F(\theta)\left[\mathbf{Tr}\left(tt^\dagger\right) - \mathbf{Tr}\left(tt^\dagger\right)^2\right], \tag{5}$$

where t is the transmission block of S matrix and

$$F(\theta) = \theta \coth(\theta), \quad \theta \equiv \frac{eV}{2k_B T}. \tag{6}$$

Equation (5) is general and valid at any temperature in the linear regime of quantum transport, including both the shot-noise power and thermal noise. Equation (5) for the noise $\boldsymbol{\mathcal{S}}$ comprises all the scattering phenomena and is valid for any S-matrix. In particular, we will consider ballistic chaotic system, i.e., QDs for which the edges are random and geometry becomes statistically irrelevant to the main cumulants of the universal phenomena of quantum transport. In the situation of universal transport, for our purposes, we introduce a stub parametrization [20] to embody the collusive effects of barriers and all pertinent decoherence fields.

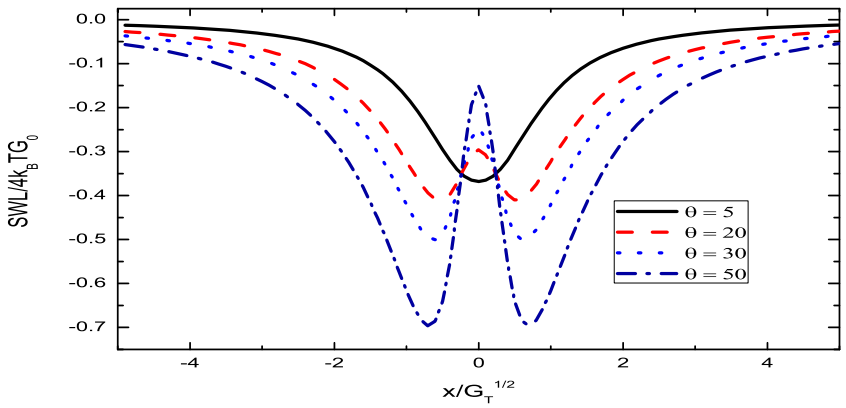

Fig. 5 Quantum interference term of noise as a function of perpendicular magnetic field. We fix $\Gamma_1 = 0.8$, $\Gamma_2 = 0.9$, $N_1 = 30$, $N_2 = 20$, $b_\perp = 5$, $b = 10$, and $a = a_\perp = 0$

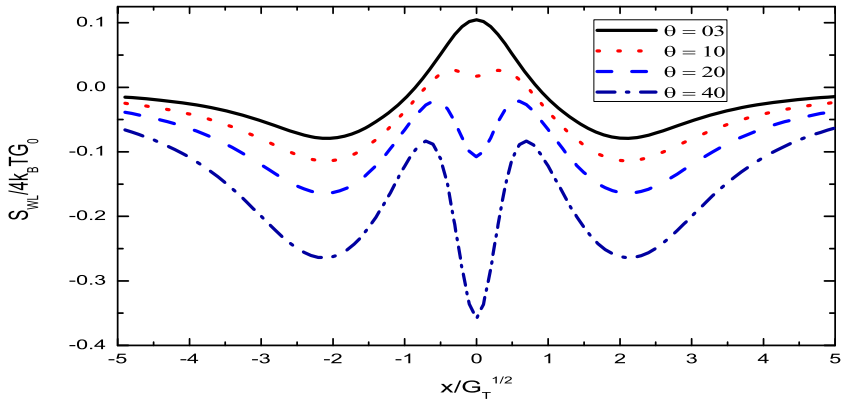

Fig. 6 Interference correction for noise as a function of magnetic field perpendicular

The stub is a fictitious small extension of the geometry of the QD, which, equivalently to external fields, enlarge the dwell time of the electron inside the QD. The stub is depicted in Fig. 1. Effect of spin imposes a unitary scattering matrix with quaternionic entries [8, 11, 15],

$$S = TU\left(1 - Q^{\dagger}RQU\right)^{-1}T^{\dagger}, \tag{7}$$

where U is a $M \times M$ unitary symmetric matrix taken from Dyson's circular orthogonal ensemble. M stands for the number of resonances of the QD, while $N = N_1 + N_2$ is the total number of open channels, also identified with the order of the S-matrix. The Q-matrix is a projection operator of order $(M - N) \times M$, while T of order $N \times M$ describes the channels-resonances couplings (barriers). Their explicit forms read $Q_{ij} = \delta_{i+N,j}$ and $T_{ij} = \text{diag}\left(i\delta_{i,j}\sqrt{\Gamma_1}, i\delta_{i+N_1,j}\sqrt{\Gamma_2}\right)$. Decoherence parameters, in the stub framework, are introduced through the quaternionic $(M - N) \times (M - N)$ unitary matrix R, defined as

$$R\left(\tau_B, \tau_{||}^{SO}, \tau_{\perp}^{SO}, \tau^Z, \tau_{\perp}^Z\right) = \exp\left[-i\left(\frac{\mathcal{H}}{M} + iV\mathbf{1}_2\right)\right], \tag{8}$$

where $\mathcal{H} \equiv \mathcal{H}\left(\tau_B, \tau_{||}^{SO}, \tau_{\perp}^{SO}, \tau^Z, \tau_{\perp}^Z\right)$ is a $(M - N) \times (M - N)$ quaternionic matrix carrying the relevant information about the symmetry breaks. The decoherence time scales, $\tau_B, \tau_{||}^{SO}, \tau_{\perp}^{SO}, \tau^Z, \tau_{\perp}^Z$ are associated, respectively, with perpendicular magnetic field, direct terms of crystals anisotropies, crossed term of crystal anisotropies, planar Zeeman field through spin-magnetic field coupling, and isolated perpendicular Zeeman field through magnetic-orbit coupling. Barriers are introduced by an $(M - N)$-dimensional matrix V, which can be constructed from the entries of matrix T. Universality of the stub method requires that the limit $M \to \infty$ be taken at the end of the calculations.

The effective Hamiltonians $\mathcal{H}(\tau_B, \tau_{SO})$ for metallic grains (isotropic model) and $\mathcal{H}\left(\tau_B, \tau_{||}^{SO}, \tau_{\perp}^{SO}, \tau^Z, \tau_{\perp}^Z\right)$ for heterostructure QD (anisotropic model) have already been thoroughly discussed in the recent literature [15]. Our presentation will focus only on the most important aspects of new results for conductance and for quantum noise in thermal crossover. Random matrix description of the crossover in the universal regime are applicable since time scales are far greater then the electron transit time τ_{erg}, i.e., $\tau_B, \tau_{SO}, \tau_{||}^{SO}, \tau_{\perp}^{SO}, \tau^Z, \tau_{\perp}^Z \gg \tau_{erg}$. The validity of the stub model is guaranteed by the requirement that both scales are of the order of the inverse mean level spacing, Δ, considering also its level broadening due to the presence of barriers. We may thus introduce the following dimensionless parameters to characterize the intensity of symmetry breaking in the system

$$x^2 \equiv \frac{2\pi\hbar}{\tau_B\Delta}, a^2 \equiv \frac{2\pi\hbar}{\tau_{SO}\Delta}, a_{\perp}^2 \equiv \frac{2\pi\hbar}{\tau_{\perp}^{SO}\Delta}, \tag{9}$$

$$b^2 \equiv \frac{2\pi\hbar}{\tau^Z\Delta}, b_{\perp}^2 \equiv \frac{2\pi\hbar}{\tau_{\perp}^Z\Delta}. \tag{10}$$

The random matrix models for the effective Hamiltonians then follow directly from general symmetry considerations. They are given by

$$\mathcal{H}_{iso} = ix\ X\ \mathbf{1}_2 + \frac{i\ a}{\sqrt{2}}\ \sum_{i=1}^{3} A_i\ \sigma_i, \tag{11}$$

for metallic grains, and

$$\mathcal{H}_{aniso} = ix\ X\ \mathbf{1}_2 + ia_{\perp}\ X\ \sigma_3 - \vec{b}\cdot\vec{\sigma} + b_{\perp}\ B\ \sigma_3 + i\ a\ \sum_{i=1}^{2} A_i\ \sigma_i. \tag{12}$$

for ballistic quantum dots patterned in GaAs heterostructures [15]. In the above equations, X and A_i $(i = 1, 2, 3)$ are real antisymmetric matrices, B is a real symmetric matrix of dimension $(M - N) \times (M - N)$, and σ_i are Pauli matrices. The matrices are uncorrelated and its entries are independent Gaussian random numbers.

3 Ensemble Averaged Quantum Conductance and Quantum Noise

We start by studying QDs at zero temperature, for which (3) yields the shot-noise power $p = \mathcal{S}/G_0 = \mathbf{Tr}\left(tt^\dagger\right) - \mathbf{Tr}\left(tt^\dagger\right)^2$. Below, we will study the quantum noise in thermal crossover and hence the asymptotic limit of the Johnson-Nyquist noise. We perform a diagrammatic perturbative expansion of the ensemble averaged conductance, $\langle \mathbf{g} \rangle = \left\langle \mathbf{Tr}\left(tt^\dagger\right) \right\rangle$, in inverse powers of N and M. The first term contributing to $\langle \mathbf{g} \rangle$ is obtained by adding ladder-type diagrams [21–23]. To perform the trace over the channel indices, we use the following identity $\mathbf{Tr}\left(R \otimes R^\dagger\right) = (M - N_1\Gamma_1 - N_2\Gamma_2)\,\mathbf{1}_2 \otimes \mathbf{1}_2$. Selecting and adding the ladder-type diagrams and using the index $\mathcal{D}$ for this contribution, we obtain

$$\left\langle \mathbf{Tr}\left(tt^\dagger\right) \right\rangle^{\mathcal{D}} = \sum_{\rho\sigma} \left\{ \left[\mathbf{Tr}\,(C_1)\,\mathbf{Tr}\,(C_2) \right] \mathcal{D} \right\}_{\rho\sigma;\sigma\rho}, \tag{13}$$

resulting in $\left\langle \mathbf{Tr}\left(tt^\dagger\right) \right\rangle^{\mathcal{D}} = 2G_1G_2/(G_1 + G_2)$ where $G_i = N_i\Gamma_i$, a semiclassical Ohm's law with G_i analogous to a classical conductance in series with $G_{j\neq i}$ in the absence of quantum interference terms. Notice that this result for ladder-type diagrams does not depend on the symmetries of the system or on the presence of external fields, being valid for both isotropic and anisotropic systems. Also $C_i = W_i T \otimes W_i^\dagger T^\dagger$, $\mathbf{Tr}(C_i) = G_i \mathbf{1}_2 \otimes \mathbf{1}_2$, $\mathcal{D} = \left[M\mathbf{1}_2 \otimes \mathbf{1}_2 - \mathbf{Tr}\left(R \otimes R^\dagger\right) \right]^{-1}$, W_1 is a $(N_1 + N_2) \times 2(N_1 + N_2)$-matrix constructed such as $(W_1)_{ij} = 1$ if $i = j$ and 0 if $i \neq j$, W_2 is a $2(N_1 + N_2) \times (N_1 + N_2)$-matrix constructed such as $(W_2)_{ij} = 1$ if $i = j + N_1 + N_2$ and 0 if $i \neq j$, in agreement with [15]. The tensor multiplications must be understood, by means of the backward multiplication rule, [11, 15] as $\left(\sigma_i \otimes \sigma_j\right)\left(\sigma_k \otimes \sigma_l\right) = \left(\sigma_i\sigma_k \otimes \sigma_l\sigma_j\right)$, and the factor 2 is due to spin degeneracy.

The next term in the expansion is called the weak-localization correction. It is composed of two contributions. The first one, denoted δg_1, is obtained from the ladder diagrams by applying the following correction to the weight [21–23] $M^{-n} \longrightarrow M^{-n} - nM^{-n-1}$. We obtain

$$\delta g_1 = -\sum_{\rho\sigma} \left\{ \left[\mathbf{Tr}\,(C_1)\,\mathbf{Tr}\,(C_2) \right] \mathcal{D}^2 \right\}_{\rho\sigma;\sigma\rho}, \tag{14}$$

or, taking spin trace, $\delta g_1 = -2G_1G_2/(G_1 + G_2)^2$ and, again, the contribution is system independent.

The second contribution to the weak localization term comes from crossed portions of Cooperon-type diagrams, which are affected by the effective hamiltonian. We obtain

$$\begin{aligned} \delta g_2 = \sum_{\rho\sigma} \Big\{ & -\left(M^{-3}\mathbf{1}_2 \otimes \mathbf{1}_2 \right) \mathbf{Tr}\left[F_L \left(\mathcal{T} f_{TT} \mathcal{T} \right) \right] \mathbf{Tr}\left[F_R \right] \\ & + \mathbf{Tr}\left[F_L \left(\mathcal{T} f_{UU} \mathcal{T} \right) F_R \right] \Big\}_{\rho\sigma;\rho\sigma}, \end{aligned} \tag{15}$$

where $\mathcal{T} = \mathbf{1}_2 \otimes \sigma_2$, and

$$F_L = C_1 + \mathbf{Tr}\left[C_1\right] \mathcal{D} \left(R^\dagger \otimes R \right), \tag{16}$$

$$F_R = C_2 + \left(R \otimes R^\dagger \right) \mathbf{Tr}\left[C_2\right] \mathcal{D}, \tag{17}$$

$$f_{UU} = \left[M\mathbf{1}_2 \otimes \mathbf{1}_2 - \mathbf{Tr}\left(R \otimes R^* \right) \right]^{-1}, \tag{18}$$

$$f_{TT} = \left(M\mathbf{1}_2 \otimes \mathbf{1}_2 \right) \mathbf{Tr}\left(R \otimes R^* \right) f_{UU}. \tag{19}$$

The superscript $*$ denotes the quaternion complex conjugation. Using (8), the conjugation rules of quaternions and taking the limit $M \longrightarrow \infty$, we obtain

$$f_{UU}^{-1} = \left(G_C + \frac{3}{2}\,a^2 \right) \mathbf{1}_2 \otimes \mathbf{1}_2 - \frac{a^2}{2} \sum_{i=1}^{3} \sigma_i \otimes \sigma_i, \tag{20}$$

for the isotropic model and

$$\begin{aligned} f_{UU}^{-1} = & \left(G_C + a_\perp^2 + 2\,a^2 + b_\perp^2 \right) \mathbf{1}_2 \otimes \mathbf{1}_2 \\ & + 2\,a_\perp\, x(\sigma_3 \otimes \sigma_0 - \sigma_0 \otimes \sigma_3) + \left(b_\perp^2 - a_\perp^2 \right) \sigma_3 \otimes \sigma_3 \\ & + i\,\vec{b}\,.\,(\vec{\sigma} \otimes \sigma_0 + \sigma_0 \otimes \vec{\sigma}) - a^2 \sum_{i=1}^{2} \sigma_i \otimes \sigma_i, \end{aligned} \tag{21}$$

for anisotropic model with $G_C = G_1 + G_2 + 2x^2$. Summing (13), (14) and (15), we find the expressions (22) and (23) for the average conductance for the isotropic and anisotropic models, respectively,

$$\left\langle \mathbf{Tr}\left(tt^\dagger\right)_{iso} \right\rangle = 2\frac{G_1G_2}{G_1 + G_2} \left[1 - \frac{(G_1\Gamma_2 + G_2\Gamma_1)}{(G_1 + G_2)} \left(\frac{1}{G_C + 2a^2} - \frac{a^2}{G_C(G_C + 2a^2)} \right) \right], \tag{22}$$

$$\begin{aligned} \left\langle \mathbf{Tr}\left(tt^\dagger\right)_{aniso} \right\rangle = 2\frac{G_1G_2}{G_1 + G_2} \Bigg[1 - \frac{(G_1\Gamma_2 + G_2\Gamma_1)}{2(G_1 + G_2)} \Bigg(& \frac{1}{G_C + 2b_\perp^2 + 4a^2} \\ & - \frac{\left(Gc + 2a^2 + 2a_\perp^2\right)^2 - 2\left(Gc + 2a^2 + 2a_\perp^2\right)\left(Gc + 2b_\perp^2\right) - 16a_\perp^2x^2 - 4b^2}{\left(Gc + 2a^2 + 2a_\perp^2\right)^2\left(Gc + 2b_\perp^2\right) + 4b^2\left(Gc + 2a^2 + 2a_\perp^2\right) - 16a_\perp^2x^2\left(Gc + 2b_\perp^2\right)} \Bigg) \Bigg]. \end{aligned} \tag{23}$$

We compared graphically (22) and (23) and found that the two have similar numerical behavior as a function of all the crossover parameters between Wigner-Dyson ensembles, including all the kind of Zeeman effects, even if the forms of the (22) and (23) are completely different. Physically, quantum interference effects produced by QD's quite distinct from the fundamental point of view display the same conductance averages. For universal conductance fluctuations and its respective variances, [15] shows that the Zeeman effect can qualitatively affect quantum properties of the system. Now, we return to the problem of investigating how the discrete nature of the charge, manifested in quantum noise, can be affected by crossover fields of anisotropic structures.

We use the diagrammatic perturbative expansion of the average shot-noise power $\langle p\rangle = \left\langle \mathbf{Tr}\left[tt^{\dagger}\left(1-tt^{\dagger}\right)\right]\right\rangle$. We can use in the crossover problem of a QD with barriers the same diagrammatic topologies typical of pure orthogonal class, which can be found in [23]. For the isotropic case, we obtain the analytical and exact result of (24)

$$\begin{aligned}\left\langle \mathbf{Tr}\left[tt^{\dagger}\left(1-tt^{\dagger}\right)\right]_{iso}\right\rangle &= 2G_1G_2\frac{G_1G_2(G_1+G_2)+G_1^3(1-\Gamma_2)+G_2^3(1-\Gamma_1)}{(G_1+G_2)^4}\\ &-\frac{4G_1^2G_2^2(G_1\Gamma_2+G_2\Gamma_1)\left[G_1(1-\Gamma_2)+G_2(1-\Gamma_1)\right]}{(G1+G2)^4}\times\left[\frac{1}{G_C^2}-\frac{3}{(G_C+2a)^2}\right]\\ &-\frac{G_1G_2(G_1\Gamma_2+G_2\Gamma_1)\left[G_1G_2(G_1+G_2)+G_1^3(3-4\Gamma_2)+G_2^3(3-4\Gamma_1)\right]}{(G_1+G_2)^5}\\ &\times\left(\frac{1}{G_C}-\frac{3}{G_C+2a^2}\right).\end{aligned} \tag{24}$$

As expected, (24) shows the total suppression of the quantum interference term in the unitary ensemble, $G_C\to\infty$. Notice also the signal inversion of the WL term when comparing the orthogonal ensemble, $a\to 0$ and $x\to 0$, with the symplectic ensemble, $a\to\infty$ and $x\to 0$. The depletion-amplification effect of the noise can also be seen in (24) when the value of the barriers transits around $\Gamma_i = 3/4$.

We also calculate the shot-noise power for anisotropic QDs in the presence of dephasing fields and obtain a general cumbersome and complicated equation, which will be studied graphically below. In particular, for $b\to 0$ and for both $a=0$ and $a_\perp\to 0$, respectively, we have the following simplifications

$$\begin{aligned}\left\langle \mathbf{Tr}\left[tt^{\dagger}\left(1-tt^{\dagger}\right)\right]_{aniso}\right\rangle &= 2G_1G_2\frac{G_1G_2(G_1+G_2)+G_1^3(1-\Gamma_2)+G_2^3(1-\Gamma_1)}{(G_1+G_2)^4}-\frac{4G_1^2G_2^2(G_1\Gamma_2+G_2\Gamma_1)\left[G_1(1-\Gamma_2)+G_2(1-\Gamma_1)\right]}{(G1+G2)^4}\\ &\times\left[\frac{1}{\left[G_C+2b_\perp^2\right]^2}-\frac{1}{\left[G_C+4a^2+2b_\perp^2\right]^2}-\frac{1}{\left[G_1+G_2+2a^2+2(x-a_\perp)^2\right]^2}-\frac{1}{\left[G_1+G_2+2a^2+2(x+a_\perp)^2\right]^2}\right]\\ &+\frac{G_1G_2(G_1\Gamma_2+G_2\Gamma_1)\left[G_1G_2(G_1+G_2)+G_1^3(3-4\Gamma_2)+G_2^3(3-4\Gamma_1)\right]}{(G_1+G_2)^5}\\ &\times\left[\frac{1}{G_C+2b_\perp^2}-\frac{1}{G_C+4a^2+2b_\perp^2}-\frac{1}{G_1+G_2+2a^2+2(x-a_\perp)^2}-\frac{1}{G_1+G_2+2a^2+2(x+a_\perp)^2}\right]\end{aligned} \tag{25}$$

$$\begin{aligned}\left\langle \mathbf{Tr}\left[tt^{\dagger}\left(1-tt^{\dagger}\right)\right]_{aniso}\right\rangle &= 2G_1G_2\frac{G_1G_2(G_1+G_2)+G_1^3(1-\Gamma_2)+G_2^3(1-\Gamma_1)}{(G_1+G_2)^4}+\frac{4G_1^2G_2^2(G_1\Gamma_2+G_2\Gamma_1)\left[G_1(1-\Gamma_2)+G_2(1-\Gamma_1)\right]}{(G1+G2)^4}\\ &\times\left[\frac{1}{G_C^2}+\frac{1}{\left[G_C+2b_\perp^2\right]^2}+\frac{4b_\perp^2\left(G_C+b_\perp^2\right)}{\left[G_C^2+2G_Cb_\perp^2+4b^2\right]^2}\right]\\ &-\frac{G_1G_2(G_1\Gamma_2+G_2\Gamma_1)\left[G_1G_2(G_1+G_2)+G_1^3(3-4\Gamma_2)+G_2^3(3-4\Gamma_1)\right]}{(G_1+G_2)^5}\\ &\times\left[\frac{1}{G_C}+\frac{1}{G_C+2b_\perp^2}+\frac{2b_\perp^2}{G_C^2+2G_Cb_\perp^2+4b^2}\right]\end{aligned} \tag{26}$$

The first terms (independent of the fields) of the sums in the equations for the noise results from the diffusions. We focus on the other terms of quantum interference correction (WL) resulting from the cooperons. For the conductance, we will denote all these terms simply by g_{WL} and, for the shot-noise power, we will denote all this terms of WL by p_{WL}. The (26) shows that only the perpendicular magnetic field x, $G_C \to \infty$, suppresses the quantum interference in shot-noise power, making the crossover among orthogonal and unitary ensembles. Other dephasing fields may annihilate the quantum interference, but only in a combination. Surprisingly, just this combined effect clearly distinguishes the types of systems, isotropic or anisotropic, by means of quantum interference.

More general physical situations require graphical studies which we consider henceforth. Figure 2 shows the ratio p_{wl}/g_{wl} between "weak localization" (WL) terms for noise and conductance in the case of symmetric contacts, $\Gamma_1 = \Gamma_2 = \Gamma$. We varied Γ from opaque limit, $\Gamma \to 0$, to the ideal contact case, $\Gamma = 1$. We set $a/\sqrt{G_T} = 1$, $x/\sqrt{G_T} = 0.5$ e $b = b_\perp = 0$. One can see that the ratio does not show a simple behavior in relation to the values of $a_\perp$ and can change in nontrivial ways the slope at the opaque limit, like an anomalous 'Fano' effect. In this regime, the presence of the Zeeman effect generates a depletion-amplification effect of the shot-noise signal analogous to the previously mentioned effect generated by the barriers. We can also notice that all curves tend to the same point in $\Gamma = 1$, showing that only in this case the ratio does not depend of the fields, despite the conjecture of [24] which shows that this ratio does not depend on crossover fields, according to the following equation:

$$\frac{p_{WL}}{g_{WL}} = -\left(\frac{N_1 - N_2}{N_1 + N_2}\right)^2. \tag{27}$$

We show that the tunneling rates play a crucial role in violating the conjecture. In the relevant case of opaque limit, when the number of channels $N_i \to \infty$ and $\Gamma_i \to 0$ with G_i finite, for example, the ratio of the weak localization correction of noise and of conductance exhibits peculiar properties, as shown in Fig. 2 and according to the following analytical equation

$$\begin{aligned}
\frac{p_{WL}}{g_{WL}} = {} & \frac{3G_1 - 2G_1G_2 + 3G_2}{(G_1+G_2)^2} - \frac{4G_1G_2}{(G_1+G_2)\left(G_C + 4a^2 + 2b_\perp^2\right)} \\
& - \frac{4G_1G_2}{(G_1+G_2)}\Big[3G_1^2 + 4G_1b_\perp^2 + 12G_1x^2 + 8a_\perp^2G_1 + 8G_1a^2 + 6G_1G_2 + 4b^2 + 4a_\perp^4 + 4G_2b_\perp^2 + 8a_\perp^2a^2 \\
& \quad + 8a^2b_\perp^2 + 8a^2G_2 + 8G_2a_\perp^2 + 4a^4 + 12x^4 + 12G_2x^2 + 8x^2b_\perp^2 + 16a^2x^2 + 3G_2^2 + 8a_\perp^2b_\perp^2\Big] \\
& \quad / \Big[8a^2b^2 + 8a_\perp^4x^2 + 8a^4b_\perp^2 + 8b^2a_\perp^2 + 8b_\perp^2a_\perp^4 - 16a_\perp^2x^2b_\perp^2 + 16a^2b_\perp^2a_\perp^2 + 16a^2a_\perp^2x^2 + 4b_\perp^2G_1G_2 \\
& \quad + 8b_\perp^2G_1x^2 + 8b_\perp^2G_1a_\perp^2 + 8b_\perp^2G_1a^2 + 8b_\perp^2G_2x^2 + 8b_\perp^2G_2a_\perp^2 + 8b_\perp^2G_2a^2 + 16b_\perp^2x^2a^2 \\
& \quad + 8a_\perp^2G_1G_2 + 8a_\perp^2G_1a^2 + 8a_\perp^2G_2a^2 + 4a^4G_1 + 4a^4G_2 + 8a^4x^2 - 16a_\perp^2x^4 + 2b_\perp^2G_1^2 \\
& \quad + 2b_\perp^2G_2^2 + 8b_\perp^2x^4 + 4a_\perp^2G_1^2 + 4a_\perp^4G_1 + 4a_\perp^2G_2^2 + 4a_\perp^4G_2 + 3G_1^2G_2 + 6G_1^2x^2 + 4G_1^2a^2 \\
& \quad + G_1^3 + G_2^3 + 8x^6 + 12G_1G_2x^2 + 8G_1G_2a^2 + 16G_1x^2a^2 + 16G_2x^2a^2 + 3G_1G_2^2 \\
& \quad + 12G_1x^4 + 6G_2^2x^2 + 4G_2^2a^2 + 12G_2x^4 + 16x^4a^2 + 4b^2G_1 + 4b^2G_2 + 8b^2x^2\Big] \\
& - \frac{4G_1G_2}{(G_1+G_2)}\Big[3G_1^2 + 8G_1b_\perp^2 + 6G_1G_2 + 4a_\perp^2G_1 + 8G_1a^2 + 12G_1x^2 + 4b^2 + 8G_2b_\perp^2 + 12G_2x^2 + 4b_\perp^4 \\
& \quad + 12x^4 + 8x^2a_\perp^2 + 4G_2a_\perp^2 + 3G_2^2 + 16x^2b_\perp^2 + 8a_\perp^2b_\perp^2 + 16a^2b_\perp^2 + 16a^2x^2 + 8a^2G_2\Big] \\
& \quad / \Big[-4b^2b_\perp^2 - 4b^2a_\perp^2 - 8b_\perp^4a_\perp^2 - 16a_\perp^2x^2b_\perp^2 + \Big(8a_\perp^4 - 12b^2 - 16G_2x^2 - 8b_\perp^4 - 16G_2b_\perp^2 - 16a_\perp^2b_\perp^2 \\
& \qquad - 32x^2a_\perp^2 - 16G_1b_\perp^2 - 32x^2b_\perp^2 - 8G_1G_2 \\
& \qquad - 16G_1x^2 - 4G_1^2 - 4G_2^2 - 16x^4\Big)a^2 \\
& \quad + \left(-16b_\perp^2 + 16a_\perp^2\right)a^4 - 4G_1b_\perp^4 + 8a^6 - 8b_\perp^2G_1G_2 - 16b_\perp^2G_1x^2 - 8b_\perp^2G_1a_\perp^2 - 16b_\perp^2G_2x^2 \\
& \quad - 8b_\perp^2G_2a_\perp^2 - 4a_\perp^2G_1G_2 - 8a_\perp^2x^4 - 4b_\perp^2G_1^2 - 4b_\perp^2G_2^2 - 16b_\perp^2x^4 - 2a_\perp^2G_1^2 - 2a_\perp^2G_2^2 - 3G_1^2G_2 \\
& \quad - 6G_1^2x^2 - G_1^3 - G_2^3 - 8x^6 - 12G_1G_2x^2 - 3G_1G_2^2 - 12G_1x^4 - 6G_2^2x^2 - 12G_2x^4 - 4b^2G_1 \\
& \quad - 4b^2G_2 - 8b^2x^2 - 8G_1x^2a_\perp^2 - 4b_\perp^4G_2 - 8b_\perp^4x^2 - 8a_\perp^2x^2G_2\Big]
\end{aligned} \tag{28}$$

Taking the limit $x \to \infty$, the (28) simplifies to the following form

$$\frac{p_{WL}}{g_{WL}} = \frac{3G_1 - 2G_1G_2 + 3G_2}{(G_1 + G_2)^2}, \tag{29}$$

showing that the perpendicular finite magnetic field also plays an essential role in the violation of conjecture placed in [24], amplified in combination with anisotropic and Zeeman fields.

One of the main results is the complete separation of the types of effects produced by the myriad of categories of universal systems. For this purpose, Fig. 3 displays the shot-noise WL term as a function of perpendicular magnetic field. We fix typical values of $\Gamma_1 = 0.8, \Gamma_2 = 0.9, N_1 = 30, N_2 = 20$, and $a/\sqrt{G_T} = 0.2$ for both isotropic and anisotropic cases. Without loss of generality, we fix $b \to 0$ and $b_\perp \to 0$ in anisotropic case. We can ascertain that the graphs of p_{WL} for isotropic and anisotropic systems are very similar when $a_\perp \to 0$, making it difficult to differentiate the physical quantum interference effects of the two kinds of QDs. We can see that the two systems show completely different behavior in the presence of the Zeeman effect that makes $a_\perp$ finite for anisotropic structures.

Now, we focus on the study of thermal noise in the crossover regime. As [25] indicates, in this regime, the effect of depletion-amplification on the shot-noise power is suppressed with the increasing of temperature, even in pure Dyson ensembles. This invites us to ask what is the combined effect of this suppression mechanism with the Zeeman effect and other crossover fields in the characterization of the WL effects. We studied the thermal crossover [25] replacing the equations for the average conductance and shot-noise in the average of the (5). Again, the result is a long and complicated equation. Without loss of generality, we study the relevant effects to the general noise by means of graphs. Firstly, we studied the effect of parallel magnetic field by means of Fig. 4 which shows the interference correction for the noise as a function of perpendicular magnetic field for finite parallel field b. We set $\Gamma_1 = 0.8, \Gamma_2 = 0.9, N_1 = 30, N_2 = 20, b_\perp = 5, \theta = 20$ (finite temperature), and $a = a_\perp = 0$ and seen subtle differences in the noise. We studied the role of $a_\perp$ compared to b, the two Zeeman fields, in the noise. We observed that the effect of $a_\perp$ is much more strong and compelling, as can be seen by comparing previous figures.

We found that the effect of θ can generate an "echo" in noise, concerning the appearance of two strong secondary peaks and inversion of the main peak [26] in the orthogonal-unitary crossover, as can be seen in Fig. 5. This figure shows quantum interference term of noise as a function of perpendicular magnetic field, where we set $\Gamma_1 = 0.8, \Gamma_2 = 0.9, N_1 = 30, N_2 = 20, b_\perp = 5, b = 10$, and $a = a_\perp = 0$.

We also observe the effect of θ in the transition "localization" and "anti-localization" for the noise. Figure 6 shows the interference correction for noise as a function of perpendicular magnetic field. We set $\Gamma_1 = 0.8, \Gamma_2 = 0.9, N_1 = 30, N_2 = 20, a_\perp = 2, a = 1$, and $b = b_\perp = 0$. We found again the "echo" and the annihilation of depletion-amplification transition with the increase of θ.

4 Discussion and Conclusions

In this paper, we present a very detailed study of the role of quantum interference in noise. We consider a wide class of crossovers between the Wigner-Dyson ensembles and between different thermal regimes. Furthermore, the crossover between ensembles take into account the parallel and perpendicular magnetic fields, the Zeeman effect, the longitudinal spin-orbit coupling caused by anisotropy in the crystal lattice, the spin-orbit coupling due to the parallel magnetic field, etc. We also take into account the effects of temperature in the reservoirs of electrons to obtain both the relevant regime of shot-noise and thermal noise of Nyquist-Johnson. We show surprising effects on depletion-amplification noise due to the controllable parameters. To connect with the modern real-time measurements, we take into account the role of tunneling barriers. Our study provides several important regimes and show a great possibility to measure [27, 28] the effect of quantum interference in nonequilibrium fluctuations in chaotic nonideal nanostructures. The conclusion that the Zeeman effect has strong phenomenological implications to the temporal fluctuations of the conductance (noise) is a useful information on spintronics for future investigations following the perspective of [29]. Another interesting future study is to investigate the role of the Zeeman effect and temperature on universal conductance fluctuations following this work and [30]. Our study also shows explicitly the effect of competition among the leading concepts of general quantum mechanics and thermodynamics as follows: interference, fluctuation-dissipation, tunneling, symmetries, and discreteness of electronic transport.

Acknowledgments This work was partially supported by CNPq, FAPESP, FACEPE, and INCT-IQ (Brazilian Agencies).

References

1. S. Gustavsson, R. Leturcq, M. Studer, I. Shorubalko, T. Ihn, K. Ensslin, D.C. Driscoll, A.C. Gossard, Surface Science Reports. **64**, 191 (2009)

2. S. Gustavsson, R. Leturcq, B. Simovic, R. Schleser, T. Ihn, P. Studerus, K. Ensslin, D.C. Driscoll, A.C. Gossard, Phys. Rev. Lett. **96**, 076605 (2006)
3. C.W.J. Beenakker, Rev. Mod. Phys. **69**, 731 (1997)
4. Y. Alhassid, Rev. Mod. Phys. **72**, 895 (2000)
5. P.A. Mello, N. Kumar, *Quantum Transport in Mesoscopic Systems* (Oxford University Press, Oxford, 2004)
6. C.H. Lewenkopf, H.A. Weidenmüller, Ann. Phys. (N.Y.) **212**, 53 (1991)
7. E. Akkermans, G. Montambaux, *Mesoscopic Physics of Electrons and Photons* (Cambridge University Press, Cambridge, 2006)
8. M.L. Mehta, *Random Matrices, 3rd Edn.* (Elsevier, Amsterdam, 2004)
9. S. Hikami, A.I. Larkin, Y. Nagaoka, Prog. Theor. Phys. **63**, 707 (1980)
10. A.V. Khaetskii, Yu.V. Nazarov, Phys. Rev. B **61**, 012639 (2000)
11. J.G.G.S. Ramos, A.L.R. Barbosa, A.M.S. Macêdo, Phys. Rev. B **84**, 035453 (2011)
12. J.A. Folk, S.R. Patel, K.M. Birnbaum, M. Marcus, C.I. Duruöz, J.S. Harris Jr., Phys. Rev. Lett. **86**, 2102 (2001)
13. B.I. Halperin, A. Stern, Y. Oreg, J.N.H.J. Cremers, J.A. Folk, C.M. Marcus, Phys. Rev. Lett., Vol. 86 (2001)
14. I.L. Aleiner, V.I. Falko, Phys. Rev. Lett. **87**, 256801 (2001)
15. J.N.H.J. Cremers, P.W. Brouwer, V.I. Fal'ko, Phys. Rev. B **68**, 125329 (2003)
16. Ya.M.. Blanter, M. Büttiker, Phys. Rep. **336**, 1 (2000)
17. P.A. Mello, N. Kumar, *Quantum Transport in Mesoscopic Systems: Complexity and Statistical Fluctuations* (Oxford University Press, Oxford, 2004)
18. M. Büttiker, Phys. Rev. Lett. **65**, 2901 (1990)
19. V. A.l. Osipov, E. Kanzieper, J. Phys. A: Math. Theor. **42**, 475101 (2009)
20. M.L. Polianski, P.W. Brouwer, J. Phys. A: Math. Gen. **36**, 3215 (2003)
21. P.W. Brouwer, C.W.J. Beenakker, J. Math. Phys. **37**, 4904 (1996)
22. J.G.G.S. Ramos, A.L.R. Barbosa, A.M.S. Macêdo, Phys. Rev. B **78**, 235305 (2008)
23. A.L.R. Barbosa, J.G.G.S. Ramos, A.M.S. Macêdo, J. Phys. A **43**, 075101 (2010)
24. B. Béri, J. Cserti, Phys. Rev. B **74**, 235314 (2006); B. Béri, J. Cserti, Phys. Rev. B **75**, 041308(R) (2007)
25. A.L.R. Barbosa, J.G.G.S. Ramos, D. Bazeia, Eurphys. Lett. **93**, 67003 (2011)
26. A.L.R. Barbosa, J.G.G.S. Ramos, D. Bazeia, Phys. Rev. B **84**, 115312 (2011)
27. S. Gustavsson, R. Leturcq, T. Ihn, K. Ensslin, M. Reinwald, W. Wegscheider, Phys. Rev. B Vol. 75 (2007)
28. Yu. Bomze, G. Gershon, D. Shovkun, L.S. Levitov, M. Reznikov, Phys. Rev. Lett. **95**, 176601 (2005)
29. J.G.G.S. Ramos, A.L.R. Barbosa, D. Bazeia, M.S. Hussein, C.H. Lewenkopf, Phys. Rev. B Vol. 86 (2012)
30. J.G.G.S. Ramos, D. Bazeia, M.S. Hussein, C.H. Lewenkopf, Phys. Rev. Lett. **107**, 176807 (2011)